

Review

Variability of the Conductance Changes Associated with the Change in the Spin State in Molecular Spin Crossover Complexes

 M. Zaid Zaz^{1,*}, Thilini K. Ekanayaka², Ruihua Cheng³ and Peter A. Dowben^{1,*} 
¹ Department of Physics and Astronomy, University of Nebraska-Lincoln, Lincoln, NE 68588-0299, USA

² Applied Materials, Santa Clara, CA 95054, USA; thilini_ekanayaka@amat.com

³ The Department of Physics, Indiana University Purdue University-Indianapolis, Indianapolis, IN 46202, USA; rucheng@iupui.edu

* Correspondence: zzaz2@huskers.unl.edu (M.Z.Z.); pdowben1@unl.edu (P.A.D.); Tel.: +1-402-472-9838 (P.A.D.)

Abstract: Here, we examine the conductance changes associated with the change in spin state in a variety of different structures, using the example of the spin crossover complex $[\text{Fe}(\text{H}_2\text{B}(\text{pz})_2)_2(\text{bipy})]$ (pz = (pyrazol-1-yl)-borate and bipy = 2,2'-bipyridine) and $[\text{Fe}(\text{Htrz})_2(\text{trz})(\text{BF}_4)]$ (Htrz = 1H-1,2,4-triazole) thin films. This conductance change is highly variable depending on the mechanism driving the change in spin state, the substrate, and the device geometry. Simply stated, the choice of spin crossover complex used to build a device is not the only factor in determining the change in conductance with the change in spin state.

Keywords: spin crossover; conductance change; substrate effects; device geometry

1. Introduction

There are a number of transition metal complexes that exhibit a reversible change in spin state, typically with temperature [1–6] but also with voltage [7], light [8–10], pressure [9–12], and other external perturbations. For Fe (II) complexes, in the diamagnetic low spin state (LS, $t_{2g}^6 e_g^0, {}^1A_1$), the lower energy t_{2g} molecular orbital is fully occupied, leaving no unpaired electrons. Conversely, in the paramagnetic high spin state (HS, $t_{2g}^4 e_g^2, {}^5T_2$), the higher energy e_g molecular orbitals become occupied, resulting in unpaired electrons [1–6]. Accompanying this spin state transition, there is often a change in conductance, sometimes by many orders of magnitude [7,13–47]. This change in conductance, associated with a change in spin state, can be voltage controlled [7,14,15,18] and when formed in a bilayer with a molecular ferroelectric a nonvolatile voltage-controlled device, based on molecular systems, is realized [7,14,17], as illustrated in Figure 1. For most practical memory applications, switching is required to be non-volatile, isothermal (near and above room temperature), bidirectional, and voltage controlled. The greater the change in conductance with the isothermal switching of the spin state, the better the device fidelity [7], but what exactly controls this on/off ratio is far from settled. The objective of this review is to show that while significant conductance changes have been observed to accompany molecular spin state switching, the magnitude of this change depends on a great many factors, not all of which are completely understood. We illustrate these points by noting the various results obtained from thin films of $[\text{Fe}(\text{H}_2\text{B}(\text{pz})_2)_2(\text{bipy})]$ (pz = (pyrazol-1-yl)-borate and bipy = 2,2'-bipyridine) and $[\text{Fe}(\text{Htrz})_2(\text{trz})(\text{BF}_4)]$ (where Htrz = 1H-1,2,4-triazole) as examples. In particular, we emphasize that switching mechanism [14], device geometry as well as contact resistance [37] greatly affect not only the on/off ratio but the conductance as well. We also point out that polymeric additives [16,45] as well as charge transfer salts [22,43,46–48] have a strong influence on the conductance and frequently on the on/off ratio as well [16,43]. While one can speculate about a mechanism for conductance change in spin crossover complexes, a definitive picture presently remains elusive as we show here. $[\text{Fe}(\text{H}_2\text{B}(\text{pz})_2)_2(\text{bipy})]$ (pz = (pyrazol-1-yl)-borate and bipy = 2,2'-bipyridine) and $[\text{Fe}(\text{Htrz})_2(\text{trz})(\text{BF}_4)]$ (where



Citation: Zaz, M.Z.; Ekanayaka, T.K.; Cheng, R.; Dowben, P.A. Variability of the Conductance Changes Associated with the Change in the Spin State in Molecular Spin Crossover Complexes. *Magnetochemistry* **2023**, *9*, 223. <https://doi.org/10.3390/magnetochemistry9110223>

Academic Editor: Talal Mallah

Received: 8 September 2023

Revised: 11 October 2023

Accepted: 24 October 2023

Published: 29 October 2023



Copyright: © 2023 by the authors. Licensee MDPI, Basel, Switzerland. This article is an open access article distributed under the terms and conditions of the Creative Commons Attribution (CC BY) license (<https://creativecommons.org/licenses/by/4.0/>).

Htrz = 1H-1,2,4-triazole) are very different but both complexes are now well studied. The $[\text{Fe}(\text{H}_2\text{B}(\text{pz})_2)_2(\text{bipy})]$ (pz = (pyrazol-1-yl)-borate and bipy = 2,2'-bipyridine) spin crossover complex is depicted in Figure 2; the spin transition for this complex occurs at around spin 120 K [14,17,49–55]. The spin crossover polymer $[\text{Fe}(\text{Htrz})_2(\text{trz})](\text{BF}_4)$ (Htrz = 1H-1,2,4-triazole) is schematically depicted in Figure 3; spin transition for this complex occurs above room temperature at around 340 K [13,16,31–34,36,38–40,45].

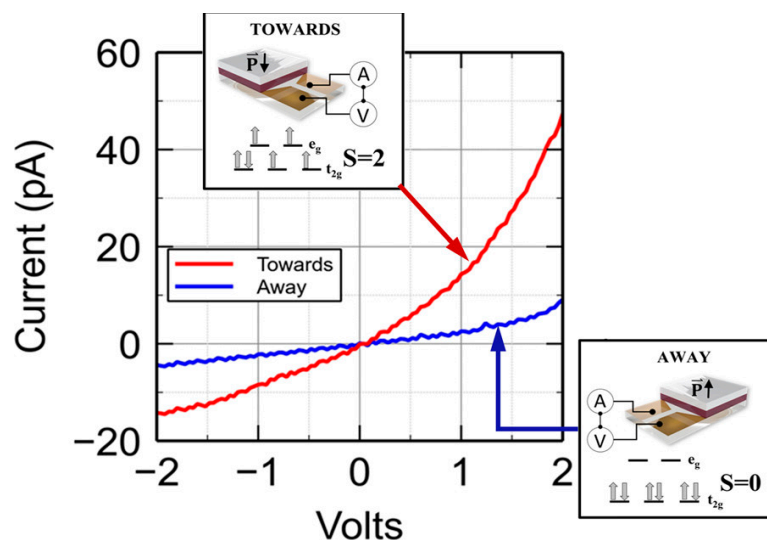


Figure 1. The change in conductance observed in a $[\text{Fe}(\text{H}_2\text{B}(\text{pz})_2)_2(\text{bipy})]$ thin film, 65 nm thick, with different ferroelectric polarization directions in an adjacent thin film of the molecular ferroelectric polyvinylidene fluoride hexafluoropropylene (PVDF-HFP). Transport measurements were taken across a device in the transistor geometry, at room temperature, with the ferroelectric layer adjacent to the SCO layer. Polarizing the ferroelectric towards the $[\text{Fe}(\text{H}_2\text{B}(\text{pz})_2)_2(\text{bipy})]$ layer results in the high spin state (nominally $S = 2$) with larger conductance. The polarization of the ferroelectric away from the $[\text{Fe}(\text{H}_2\text{B}(\text{pz})_2)_2(\text{bipy})]$ layer leads to the low spin state, a diamagnetic $S = 0$ state, and lower conductance. Reproduced from [14], with permission from the American Chemical Society.

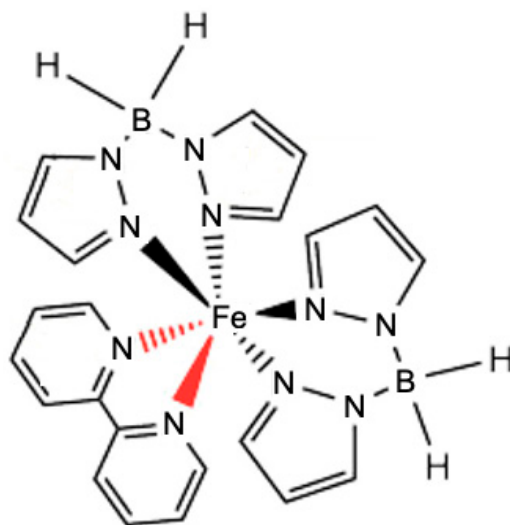


Figure 2. The $[\text{Fe}(\text{H}_2\text{B}(\text{pz})_2)_2(\text{bipy})]$ molecular spin crossover complex, discussed herein, depicted schematically.

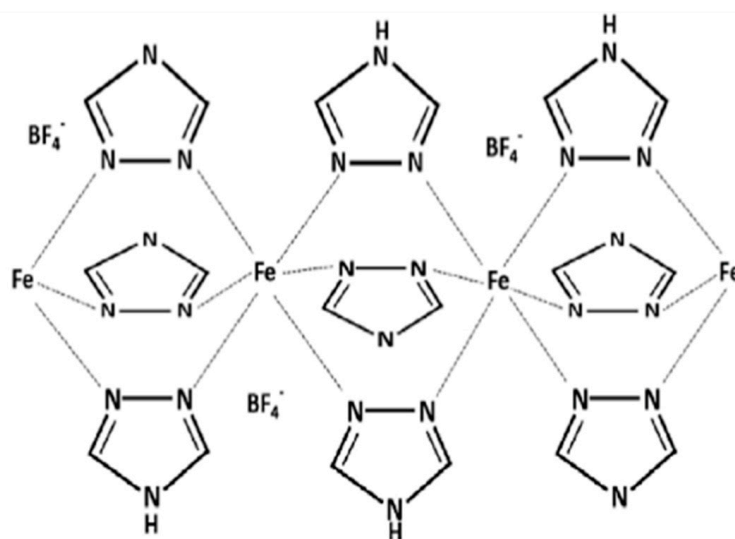


Figure 3. The $[\text{Fe}(\text{Htrz})_2(\text{trz})](\text{BF}_4)$ spin crossover polymer, also discussed herein, depicted schematically. Adapted from [16] with permission from Elsevier.

2. Variability of Conductance Change

2.1. Thermal- versus Voltage-Controlled Switching

It has been demonstrated that thin films of $[\text{Fe}\{\text{H}_2\text{B}(\text{pz})_2\}_2(\text{bipy})]$ can be driven through a spin crossover transition if the polarization of an underlying ferroelectric substrate is switched using an applied voltage [7,14,17]. This switching between the high spin state and the low spin state occurs not only for the molecules in the immediate proximity of the ferroelectric but also propagates up to 24 molecular layers [56]. For thicker $[\text{Fe}\{\text{H}_2\text{B}(\text{pz})_2\}_2(\text{bipy})]$ films on an organic ferroelectric, switching may be incomplete with the change in ferroelectric polarization, which translates to a lower on/off ratio [14]. Furthermore, the notion that voltage-controlled switching in thicker films is incomplete is supported by spectroscopic measurements [14,49]. Figure 1 shows the on and off state current versus voltage, $I(V)$, characteristics of a 65 nm thick $[\text{Fe}\{\text{H}_2\text{B}(\text{pz})_2\}_2(\text{bipy})]$ film on an organic ferroelectric polyvinylidene fluoride hexafluoropropylene (PVDF-HFP) substrate, which corresponds to a change in the high spin state occupancy in the $[\text{Fe}\{\text{H}_2\text{B}(\text{pz})_2\}_2(\text{bipy})]$ film. In this molecular heterolayer device geometry, an on/off ratio of about six is achieved through voltage-controlled switching of the ferroelectric, although it is known that the ferroelectric polarization retention is not always guaranteed [49]. In a similar thin film geometry without the adjacent ferroelectric layer, however, a significant improvement in the on/off ratio is observed when the spin state is switched through temperature variation, as more complete molecular spin state switching is assured. As seen in Figure 4, the leakage current is drastically reduced, consistent with a more complete spin state transition with temperature.

Similar changes in the current across the $[\text{Fe}(\text{H}_2\text{B}(\text{pz})_2)_2(\text{bipy})]$ thin film, which are far more characteristic of a full change in the spin state instead of a partial change in the spin state, can be accomplished by an electric field if we ensure that the entire $[\text{Fe}(\text{H}_2\text{B}(\text{pz})_2)_2(\text{bipy})]$ thin film is influenced by the applied electric field. Such is the case for a $[\text{Fe}(\text{H}_2\text{B}(\text{pz})_2)_2(\text{bipy})]$ thin film in a diode-type structure, as seen in Figure 5. In this case, the currents for the “on” state are some 10^3 to 10^4 times larger than seen for the “off” state [7].

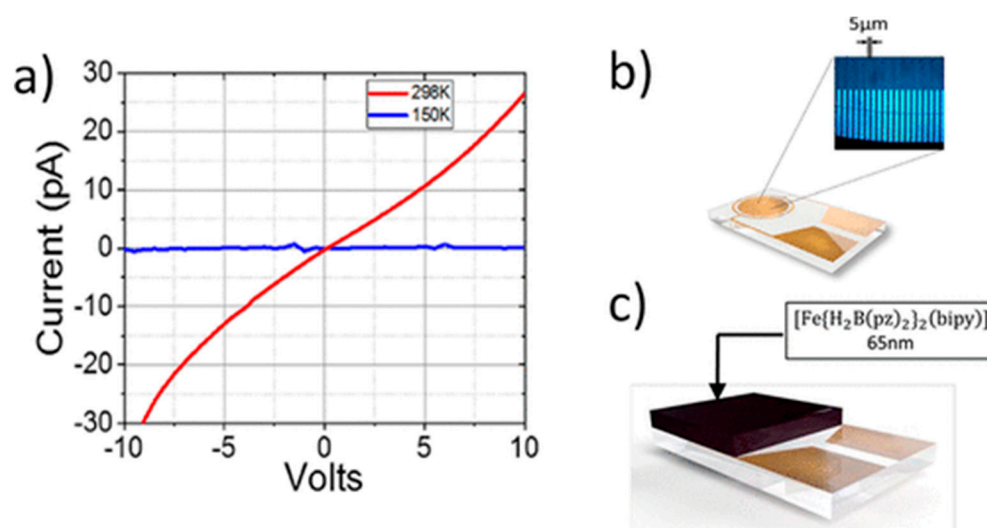


Figure 4. The differences in conductance for a 65 nm thick $[\text{Fe}(\text{H}_2\text{B}(\text{pz})_2)_2(\text{bipy})]$ thin film in the high spin taken at 298 K (red) versus the low spin dominated state with the current measured at 150 K (a). The interdigitated fingers, with a spacing of 5 μm , used as the basis for the transport measurement are indicated in (b) with the $[\text{Fe}(\text{H}_2\text{B}(\text{pz})_2)_2(\text{bipy})]$ thin film deposited directly on patterned electrodes as in (c). Reproduced from [14], with permission from the American Chemical Society.

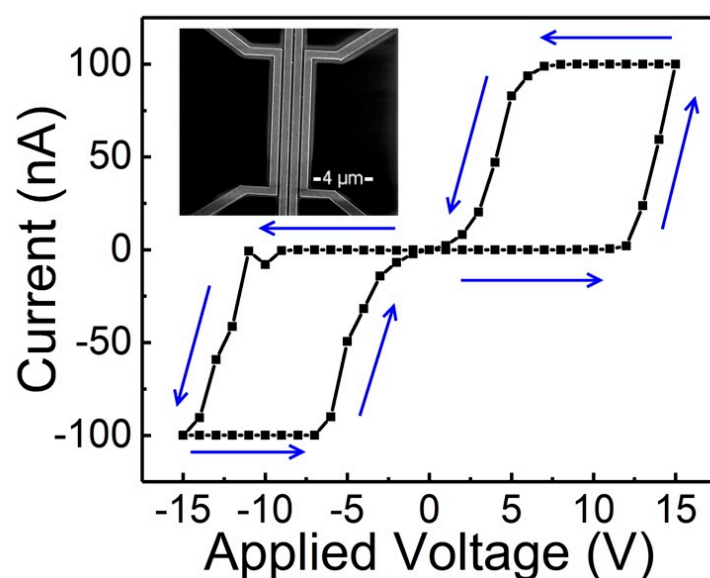


Figure 5. Evidence of conductance changes, with applied voltage, of a 20 nm $[\text{Fe}(\text{H}_2\text{B}(\text{pz})_2)_2(\text{bipy})]$ thin film deposited on top of 200 nm thick croconic acid thin film. Longitudinal voltage was applied on different junctions and the measurement was taken at room temperature. With the very small gap between electrodes, the ferroelectric fails to lock the changing conductance state of $[\text{Fe}(\text{H}_2\text{B}(\text{pz})_2)_2(\text{bipy})]$ at zero applied voltage. In this device, the measured width and pitch of the smallest portion of the electrodes were 550 nm and 700 nm, respectively. Reproduced from [7], with permission from MDPI.

2.2. The Effect of the Device Structure and Underlying Substrate

The on/off ratio is not only a function of the spin crossover material and the switching mechanism, but the underlying device geometry also seems to play a significant role. As discussed above, in the diode geometry, more complete switching is seen with an applied voltage for a $[\text{Fe}(\text{H}_2\text{B}(\text{pz})_2)_2(\text{bipy})]$ thin film (Figure 5) than in the transistor-like geometry (Figure 1). For the $[\text{Fe}(\text{Htrz})_2(\text{trz})](\text{BF}_4)$ spin crossover polymer complex, several studies report an on/off ratio ranging from 2 to 300 depending on whether a graphene-based

diode-like device geometry was used or an Au/SCO/Au type arrangement was used [37] for the $[\text{Fe}(\text{HB}(\text{tz})_3)_2]$ ($\text{tz} = 1,2,4\text{-triazol-1-yl}$) complex. In general, multilayer junctions lead to a higher on/off ratio as compared to a diode-like geometry [37,44]. The effect of contact resistance in the variability of conductance changes observed for different device geometries cannot be ruled out, as is demonstrated in the case of $[\text{Fe}(\text{HB}(\text{tz})_3)_2]$ ($\text{tz} = 1,2,4\text{-triazol-1-yl}$) in an indium tin oxide (ITO)/100 nm $[\text{Fe}(\text{HB}(\text{tz})_3)_2]/\text{Al}$ junction, where an on/off ratio of 50 was observed. This on/off ratio was shown to be enhanced up to 400 in a similar device geometry of the ITO/100 nm SCO/Ca junction [37]. Similarly, an on/off ratio of 1500 has been reported for $[\text{Fe}(\text{Htrz})_2(\text{trz})](\text{BF}_4)$ [33] in a structure involving multiple Au dots in an array, which is much larger than is typical for $[\text{Fe}(\text{Htrz})_2(\text{trz})](\text{BF}_4)$, as summarized in Table 1. Nevertheless, even for comparable electrode and spin crossover materials, the effects of device geometry remain significant [44].

Table 1. Summary of the variation of conductance changes across the spin crossover transition for $[\text{Fe}(\text{Htrz})_2(\text{trz})](\text{BF}_4)$. Conductance values and ratios were determined at 15 V [32,40], 1 V [39], 20 V [36], 10 V [31], 0.4 V [34], 1.5 to 2 V [38], and 1.2 V [31], while for [13], information as to the bias voltage was not clear.

On State	On/Off Ratio	On-State Current (A)	Off-State Current (A)	Switching Mechanism	Reference
Low spin state	380	1.9×10^{-9}	5×10^{-12}	Temperature controlled	[32]
Low spin state	8	-	-	Temperature controlled	[39]
Low spin state	2	2×10^{-13}	1×10^{-13}	Temperature controlled	[13]
Low spin state	1.6	1×10^{-10}	0.5×10^{-10}	Temperature controlled	[36]
High spin state	11	5.5×10^{-9}	0.5×10^{-9}	Temperature controlled	[31]
High spin state	6	6×10^{-11}	1×10^{-11}	Temperature controlled	[40]
High spin state	1.7	9.2×10^{-10}	5.2×10^{-10}	Temperature controlled	[34]
High spin state	1.5	6×10^{-8}	4×10^{-8}	Photo induced	[38]
High spin state	1.5	-	-	Temperature controlled	[41]

It has been fairly well established that the underlying substrate wields a strong influence on the spin state stability of spin crossover thin films [57]. As a key example, as mentioned above, there exists compelling evidence that the polarization direction of an adjacent molecular ferroelectric, like polyvinylidene fluoride hexafluoropropylene (PVDF-HFP), has a significant influence on the spin state of a $[\text{Fe}(\text{H}_2\text{B}(\text{pz})_2)_2(\text{bipy})]$ spin crossover thin film to a film thickness of 24 molecules [56] or about 25 to 30 nm thick. In fact, the influence of the substrate is not only limited to spin state stability, but also extends to the magnitude of the conductance itself [43,49,57].

It is important to realize that the substrate affects not only the spin state and stability of that spin state with temperature, but also the actual conductance. This is especially intriguing in the case of ferroelectric substrates because these substrates can “lock” the spin crossover molecular thin film in the low spin state [57], which is frequently the low conductance state. Despite this, it can be seen that ferroelectric substrates lead to an increase in conductance. As an example, the effect of ferroelectric polyvinylidene fluoride hexafluoropropylene (PVDF-HFP) on the conductance in both the high spin (HS) and low

spin (LS) states of $[\text{Fe}(\text{H}_2\text{B}(\text{pz})_2)_2(\text{bipy})]$ thin films is illustrated in Figure 6. This enhanced conductance effect cannot arise by the mere presence of the ferroelectric substrate, as the substrate by itself is a strong dielectric. This also cannot just be an interface effect, as it propagates at least up to 24 molecular layers, but also because the change in the measured current is large. Although the mechanism for this enhancement of conductance is not known, we suggest that the effect arises from changes to the $[\text{Fe}(\text{H}_2\text{B}(\text{pz})_2)_2(\text{bipy})]$ molecular packing within the thin film resulting in a significant change in the cooperative effects.

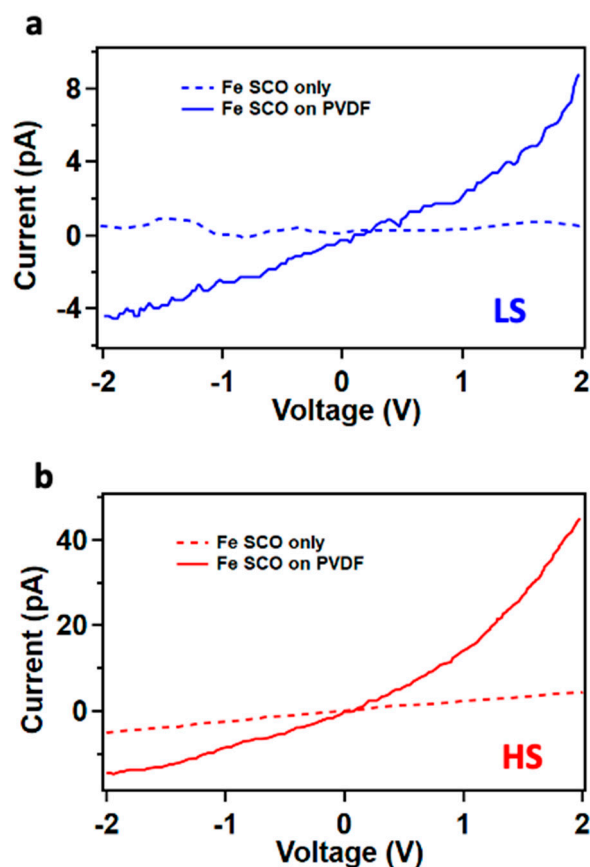


Figure 6. The current–voltage characteristics observed in (a) low spin (LS) and (b) high spin (HS) states for thin films of $[\text{Fe}(\text{H}_2\text{B}(\text{pz})_2)_2(\text{bipy})]$ both on its own and on a polyvinylidene fluoride hexafluoropropylene (PVDF-HFP) substrate. Transport measurements for the low spin state and high spin state of $[\text{Fe}(\text{H}_2\text{B}(\text{pz})_2)_2(\text{bipy})]$ thin films were conducted at temperatures of 150 K and 298 K respectively. Meanwhile, for the $[\text{Fe}(\text{H}_2\text{B}(\text{pz})_2)_2(\text{bipy})]$ film on PVDF-HFP, the measurements were carried out with the organic ferroelectric polyvinylidene fluoride hexafluoropropylene (PVDF-HFP) polarized away from the $[\text{Fe}(\text{H}_2\text{B}(\text{pz})_2)_2(\text{bipy})]$ film (representing the low spin state), and conversely, polarized towards the $[\text{Fe}(\text{H}_2\text{B}(\text{pz})_2)_2(\text{bipy})]$ film (indicating the high spin state) at room temperature. Adapted from [43,49] under the Institute of Physics Publishing creative commons attribution license.

Cooperative effects are known to have significant effects on the spin state transition in spin crossover complexes and the hysteresis loops observed in spin state transitions are directly related to these effects [6,10,58–67]. It is natural to expect that the cooperative effects are also a function of the molecular packing. Molecular packing is known to be strongly affected by the film growth process [68,69]. In fact, for molecular films, the film growth processes have a significant impact on the conductance as well as mobility [70–72]. Similar effects can be expected for spin crossover materials as well. At present, however, necessary systematic studies to draw reliable conclusions as to how deposition might affect conductance or device performance do not exist. Robust conclusions about the effect of deposition methods on the conductance of spin crossover thin films cannot be drawn from

the existing literature as one would have to first eliminate variability introduced by device design, solvent effects, substrate effects, and film thickness to make a rigorous assessment of the impact of the choice of deposition method.

3. Influence of Additives

As noted at the outset, the on-state resistance and leakage current in spin crossover-based devices, among other properties [16,22,43,45–48,50,51,63], are known to be influenced by the addition of conducting polymers [16,45] as well as charge transfer salts [22,43,46–48,63]. As an example, when the $[\text{Fe}(\text{Htrz})_2(\text{trz})](\text{BF}_4)$ spin crossover complex is formed into a composite with a semiconducting polymer-like polyaniline, the on-state resistance is reduced to less than $1 \Omega \cdot \text{cm}$ [45]. The effect of semiconducting additives is much more nuanced, however, than meets the eye at first glance. It was found that $[\text{Fe}(\text{Htrz})_2(\text{trz})](\text{BF}_4)$ plus polyaniline composites exhibit a wildly varying on/off ratio depending on the doping routes and synthesis of the polyaniline additive [16]. The polyaniline additive synthesized from the emeraldine salt form led to a higher on/off ratio and a significantly reduced leakage current as compared to the one synthesized from the emeraldine base form. Not only did the on/off current ratios vary, but the on-state current obtained using the emeraldine salt form was significantly larger than what was obtained using the emeraldine base form [16]. The addition of organic semiconducting polymers can lead to an enhancement of conductance but depends significantly on the polymer chosen to be mixed with the spin crossover [45].

The effect of mixing a charge transfer organic complex with a spin-crossover complex is also highly variable [43,46,51]. For $[\text{Fe}(\text{H}_2\text{B}(\text{pz})_2)_2(\text{bipy})]$, when an organic acceptor molecule 7,7,8,8-tetracyanoquinodimethane (TCNQ) is used as an additive, the complex is locked mostly in the low spin state but the conductance at room temperature is enhanced over the unalloyed $[\text{Fe}(\text{H}_2\text{B}(\text{pz})_2)_2(\text{bipy})]$ [43]. Polymeric and molecular additives also influence drift carrier lifetime as well as carrier mobility. Devices fabricated from $[\text{Fe}(\text{Htrz})_2(\text{trz})](\text{BF}_4)$ with a polyaniline additive feature a drift carrier lifetime more than 10–100 micro-seconds [16]. The enhancement of the drift carrier lifetime is even more remarkable in cases where TCNQ was mixed with $[\text{Fe}(\text{H}_2\text{B}(\text{pz})_2)_2(\text{bipy})]$ and an extremely long drift carrier lifetime of the order of 0.5 s was observed [43]. Thus, while molecular and polymeric additives can enhance conductance and carrier lifetime significantly, they also perturb the bistability of the spin state significantly, as seen in the case of $[\text{Fe}(\text{H}_2\text{B}(\text{pz})_2)_2(\text{bipy})]$ combined with TCNQ [43] where the spin state was seen to be locked in one spin state with the addition of some other zwitterion species [50–52].

4. The Conductance Change Mechanism

In many instances, the conductance changes accompanying the spin state transition in SCO complexes can be understood by considering the electronic structure changes occurring in tandem with the spin state change [14,17,49–53,56,73–78]. It is known that in the low spin state, the energy difference between the highest occupied molecular orbital (HOMO) and the lowest unoccupied molecular orbital (LUMO) is large enough to allow the electrons to pair up in the HOMO, leaving the LUMO empty. This is analogous to a large band gap in conventional semiconductors. In the high spin state, this HOMO–LUMO gap shrinks, and some states in the nominally unoccupied in the low spin state become occupied [13,14,17,49–53,56,75–78]. This is analogous to a narrowing of the band gap in conventional semiconductors. However, it is to be noted that molecular systems cannot be directly compared to semiconductors as the conventions of band bending do not apply very well especially if the molecules are charge neutral and the molecular films are not doped [79,80].

Changes in the HOMO–LUMO gap have been observed in optically-induced transitions in $[\text{Fe}(\text{H}_2\text{B}(\text{pz})_2)_2(\text{bipy})]$ [49] and other spin crossover complexes, while changes in the unoccupied electronic structure can be noted in the X-ray absorption spectroscopy (XAS) of $[\text{Fe}(\text{H}_2\text{B}(\text{pz})_2)_2(\text{bipy})]$ thin films [14,17,49–53,75–78], as illustrated in Figure 7. The observation that is characteristic and important to the discussion here is that a new feature

at lower photon energy emerges. This emerging feature at a lower photon energy indicates unoccupied states in the low energy t_{2g} orbitals that become partially unoccupied in the high spin state. This higher photon energy feature is indicative of unoccupied states in the higher energy e_g orbitals. Similarly, the conduction band appears closer to the Fermi level in inverse photoemission when the molecular thin film is in the high spin state [56], as seen in Figure 8. In both inverse photoemission (Figure 8) and X-ray absorption (Figure 7), the conduction band is indeed closer to the Fermi level. In the light of this discussion, one would expect the conductance in the high spin state should be enhanced as compared to the low spin state, owing to the narrowing of the band gap, as suggested elsewhere [23,56]. However, problems with this rationale based on a changing conductance associated with a changing band gap quickly emerge.

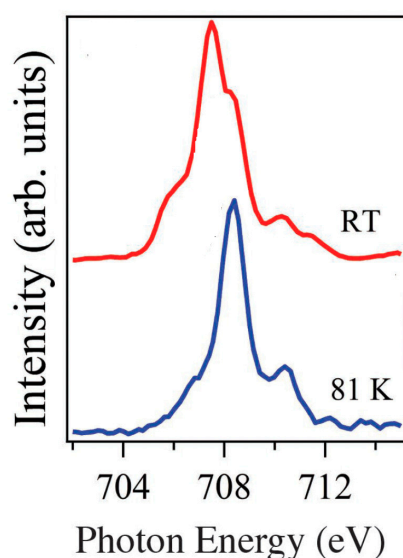


Figure 7. The temperature dependent X-ray absorption spectra of the $[\text{Fe}\{\text{H}_2\text{B}(\text{pz})_2\}_2(\text{bipy})]$ spin crossover complex. The spectrum obtained at room temperature (300 K), depicted by the red curve, signifies the complex being in the high spin state. In contrast, the blue curve representing the spectrum obtained at 81 K indicates the complex being in the low spin state. Adapted from [52] with permission from John Wiley and sons.

First among the problems with using this rationale is that for the $[\text{Fe}\{\text{H}_2\text{B}(\text{pz})_2\}_2(\text{bipy})]$ spin crossover, the band gap is not trivial (several eV). Adding to the contention that the changing band gap does not address the changing conductivity of a molecular spin crossover thin film, there are several complexes, including $[\text{Fe}(\text{Htrz})_2(\text{trz})](\text{BF}_4)$, where several studies [13,16,32,36,39,42] have reported that the low spin state has a significantly enhanced conductance compared to the high spin state. It is to be noted that other studies [31,32,38,40,41,45] have reported the opposite behavior in $[\text{Fe}(\text{Htrz})_2(\text{trz})](\text{BF}_4)$, where the high spin state has the higher conductance, as is the case for $[\text{Fe}\{\text{H}_2\text{B}(\text{pz})_2\}_2(\text{bipy})]$ discussed above. The variability of the conductance changes across the spin state transition for $[\text{Fe}(\text{Htrz})_2(\text{trz})](\text{BF}_4)$ is summarized in Table 1, and as noted above, the variability is significant. As seen in the table, not only does the spin state determine conductance, but the switching mechanism plays an important role as well. In addition to the examples mentioned in Table 1, an on/off ratio of 1500 was reported for $[\text{Fe}(\text{Htrz})_2(\text{trz})](\text{BF}_4)$ [33] and, as mentioned above, this on/off ratio is not really comparable to the examples mentioned in the table because this is in a multi-junction device. This suggests there are material issues affecting the spin crossover molecular thin film conductance changes across the spin transition, and this may include the film growth methodology and possibly the molecular polytype [16]. Just the same, the currents in the high spin state for $[\text{Fe}\{\text{H}_2\text{B}(\text{pz})_2\}_2(\text{phen})]$ films [26] and $[\text{Fe}(\text{HB}(\text{tz})_3)_2]$ films [27,37] are lower than the measured currents for the low spin state. Thus, we conclude that the conductance change across a spin transition is

not merely due to the narrowing and widening of the HOMO–LUMO gap. In addition, other factors that influence the conductance changes associated with the spin state in spin crossover molecular thin film remain far from established. It is known that the applicable correlation energy (the Hubbard on-site potential) in the high spin state is wildly different from the low spin state [53], and while this almost certainly affects conductivity, the relative significance is not yet clear. Furthermore, an applied external magnetic field is seen to affect the spin state transition for $\text{Fe}(\text{H}_2\text{B}(\text{pz})_2)_2(\text{bipy})$ [75,77], so it is entirely plausible that there may be magneto-capacitance effects as well.

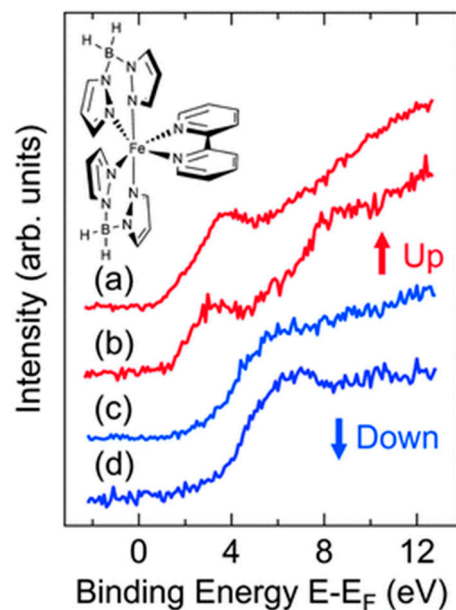


Figure 8. The inverse photoemission spectra obtained from thin films of $[\text{Fe}(\text{H}_2\text{B}(\text{pz})_2)_2(\text{bipy})]$ layered onto a ferroelectric poly-vinylidene fluoride—trifluoroethylene substrate, (a,c) show spectra obtained from $[\text{Fe}(\text{H}_2\text{B}(\text{pz})_2)_2(\text{bipy})]$ layers consisting of 25 molecules, while (b,d) show spectra corresponding to $[\text{Fe}(\text{H}_2\text{B}(\text{pz})_2)_2(\text{bipy})]$ layers spanning 10 molecular layers. The blue curves delineate instances where the ferroelectric substrate’s polarization is oriented away from the spin crossover thin film, representing the low spin state. Conversely, the red curves portray situations where the ferroelectric substrate’s polarization is directed towards the spin crossover thin film, characterizing the high spin state. Adapted from [56] with permission from the Royal Society of Chemistry.

It should be noted that the conductance changes across the spin transition are significant, thus optical absorption becomes an unreliable indicator of the band gap. As previously noted, in X-ray absorption and inverse photoemission there are strong indicators that the band gap is smaller in the high spin state than for the low spin state in $[\text{Fe}(\text{H}_2\text{B}(\text{pz})_2)_2(\text{bipy})]$ thin films in X-ray absorption [14,17,49–53,75–78] and inverse photoemission [56], a superficial inspection of the optical spectroscopy changes across the spin state transition suggests the opposite [49]. Of course, optical absorption is subject to selection rules, and a good (or better) conductor would lead to decreased interaction with the photo-hole shifting optical absorption to shorter wavelengths (higher photon energies) [81].

5. Conclusions and Outlook

Being able to control the spin state of a spin crossover molecular thin film device isothermally with voltage is vital to realizing future spintronic devices and low-power molecular memory devices [7]. Interfacial interactions seem to provide a mechanism for stabilizing a spin state well above (low spin) and below (high spin) the spin transition temperature [7,14,17,49,56,57]. The nonvolatile stabilization of the spin state, in the case of ferroelectric substrates, is shown to be amenable to modulation by an applied voltage [7,14,17,49] enabling bi-directional isothermal spin state switching. The isothermal

spin state switching is evident in spectroscopy [14,17,49] as well as transport measurements [14,17], and confirmed by magnetometry [56]. In light of the fact that the on/off ratio of the measured currents in spin crossover molecular devices seems to be sensitive to the device geometry as well as the spin state switching methodology [7,14,49] and molecular additives as discussed above, it becomes imperative to map out the dependence of conductance change and the on/off ratio on the factors that influence the conductance change. Some of these factors, namely the completeness of the spin state change or stated differently, the fraction of molecules that undergo a spin state change, influence of the substrate, the molecular packing and molecular polytype, and possibly changing cooperative effects, have been identified here. It is to be noted that film growth methodology as well as the device fabrication processes very likely play a role, but systematic studies, allowing an assessment of one parameter that affects conductance separately from the other issues that affect device performance, are almost nonexistent at present. Knowing the possible device architectures [44], a demonstration of conductance change is simply not enough. It is now well established that polymer additives and charge transfer salts have an impact on the spin crossover as well as the electronic transport properties in spin crossover molecular devices [14,22,43,46,47]; it is important to explore how the additives impact voltage-controlled switching. In summary, the choice of spin crossover complex affects the overall conductance, but other factors such as the film thickness, choice of substrate, and underlying device geometry seem to have a strong influence as well. The element of surprise is not so much that the substrate influences a thin film of spin crossover molecules, but that in many instances, the influence of the substrate extends far from the interface, affecting not just those molecules most adjacent but indeed well beyond [14,49,56,57].

It is noteworthy that the carrier mobilities in organic semiconductors are quite low, $1.3 \text{ cm}^2 \text{ v}^{-1} \text{ s}^{-1}$ [70–72], while carrier mobilities are substantially higher in spin crossover molecular films [16]. The fact that spin crossover molecules have any carrier mobility at all is very surprising to begin with. These molecules are often charge neutral and exhibit a highest occupied to lowest unoccupied molecular orbital gap. On this basis, one would expect there to be no carriers at all. So, what is the origin of charge carriers in these systems and what is the mechanism for conduction? Little is known about the nature of charge carriers (electrons or holes), the origin of charge carriers (metal or ligand contributed), and the conduction mechanisms. This understanding is needed to put all of the known and likely variables that affect device performance into a unified context.

Author Contributions: Conceptualization, M.Z.Z., T.K.E. and P.A.D.; methodology, M.Z.Z. and P.A.D.; validation, R.C.; formal analysis, M.Z.Z. and T.K.E.; investigation, M.Z.Z.; resources, R.C. and P.A.D.; data curation, M.Z.Z. and T.K.E.; writing—original draft preparation, M.Z.Z.; writing—review and editing, M.Z.Z., T.K.E., R.C. and P.A.D.; visualization, M.Z.Z.; supervision, R.C. and P.A.D.; project administration, R.C. and P.A.D.; funding acquisition, P.A.D. and R.C. All authors have read and agreed to the published version of the manuscript.

Funding: This work was supported by the National Science Foundation through NSF-DMR 2317464.

Acknowledgments: The authors thank Guanhua Hao, Aaron Mosey, Ashley S. Dale, Xuanyuan Jiang, Jian Zhang, Alpha T. N'Diaye, Xiaoshan Xu, Jared P. Phillips, Saeed Yazdani, E. Zurik, Xin Zhang, Esha Mishra, Luis G. Rosa, Bernard Doudin, Xuanyuan Jiang, Xiaoshan Xu, and Andrew Yost who contributed to this work.

Conflicts of Interest: The authors declare no conflict of interest.

References

1. Gütlich, P.; Goodwin, H.A. (Eds.) *Spin Crossover in Transition Metal Compounds I*; Springer: Berlin/Heidelberg, Germany, 2004; Volume 233, ISBN 978-3-540-40394-4.
2. Létard, J.-F.; Guionneau, P.; Goux-Capes, L. Towards Spin Crossover Applications. In *Spin Crossover in Transition Metal Compounds III*; Springer: Berlin/Heidelberg, Germany, 2004; Volume 235, pp. 221–249. ISBN 978-3-540-40395-1.
3. Gütlich, P. Spin Crossover—Quo Vadis? *Eur. J. Inorg. Chem.* **2013**, *2013*, 581–591. [[CrossRef](#)]

4. Halcrow, M.A. (Ed.) *Spin-Crossover Materials: Properties and Applications*; John Wiley & Sons: Chichester, UK, 2013; ISBN 978-1-118-51931-8.
5. Senthil Kumar, K.; Ruben, M. Emerging Trends in Spin Crossover (SCO) Based Functional Materials and Devices. *Coord. Chem. Rev.* **2017**, *346*, 176–205. [[CrossRef](#)]
6. Bousseksou, A.; Molnár, G.; Salmon, L.; Nicolazzi, W. Molecular Spin Crossover Phenomenon: Recent Achievements and Prospects. *Chem. Soc. Rev.* **2011**, *40*, 3313. [[CrossRef](#)] [[PubMed](#)]
7. Ekanayaka, T.K.; Hao, G.; Mosey, A.; Dale, A.S.; Jiang, X.; Yost, A.J.; Sapkota, K.R.; Wang, G.T.; Zhang, J.; N'Diaye, A.T.; et al. Nonvolatile Voltage Controlled Molecular Spin-State Switching for Memory Applications. *Magnetochemistry* **2021**, *7*, 37. [[CrossRef](#)]
8. Ekanayaka, T.K.; Maity, K.; Doudin, B.; Dowben, P.A. Dynamics of Spin Crossover Molecular Complexes. *Nanomaterials* **2022**, *12*, 1742. [[CrossRef](#)]
9. Chorazy, S.; Charytanowicz, T.; Pinkowicz, D.; Wang, J.; Nakabayashi, K.; Klimke, S.; Renz, F.; Ohkoshi, S.-I.; Sieklucka, B. Octacyanidorhenate (V) Ion as an Efficient Linker for Hysteretic Two-Step Iron (II) Spin Crossover Switchable by Temperature, Light, and Pressure. *Angew. Chem. Int. Ed.* **2020**, *59*, 15741–15749. [[CrossRef](#)] [[PubMed](#)]
10. Real, J.A.; Gaspar, A.B.; Muñoz, M.C. Thermal, Pressure and Light Switchable Spin-Crossover Materials. *Dalton Trans.* **2005**, *12*, 2062–2079. [[CrossRef](#)]
11. Galet, A.; Gaspar, A.B.; Agusti, G.; Muñoz, M.C.; Levchenko, G.; Real, J.A. Pressure effect investigations on the spin crossover systems {Fe[H₂B(pz)₂]₂(bipy)} and {Fe[H₂B(pz)₂]₂(phen)}. *Eur. J. Inorg. Chem. Short Commun.* **2006**, *2006*, 3571–3573. [[CrossRef](#)]
12. Orlov, Y.S.; Nikolaev, S.V.; Ovchinnikov, S.G. Magnetic Properties and Spin Crossover in Transition Metal Oxides with D⁵ Ions at High Pressures. *J. Exp. Theor. Phys.* **2019**, *129*, 1062–1069. [[CrossRef](#)]
13. Rotaru, A.; Gural'skiy, I.A.; Molnár, G.; Salmon, L.; Demont, P.; Bousseksou, A. Spin State Dependence of Electrical Conductivity of Spin Crossover Materials. *Chem. Commun.* **2012**, *48*, 4163–4165. [[CrossRef](#)]
14. Mosey, A.; Dale, A.S.; Hao, G.; N'Diaye, A.; Dowben, P.A.; Cheng, R. Quantitative Study of the Energy Changes in Voltage-Controlled Spin Crossover Molecular Thin Films. *J. Phys. Chem. Lett.* **2020**, *11*, 8231–8237, Correct in *J. Phys. Chem. Lett.* **2021**, *12*, 2463. [[CrossRef](#)]
15. Ruiz, E. Charge Transport Properties of Spin Crossover Systems. *Phys. Chem. Chem. Phys.* **2014**, *16*, 14–22. [[CrossRef](#)]
16. Mishra, E.; Ekanayaka, T.K.; McElveen, K.A.; Lai, R.Y.; Dowben, P.A. Evidence for Long Drift Carrier Lifetimes in [Fe(Htrz)₂(trz)](BF₄) plus Polyaniline Composites. *Org. Electron.* **2022**, *105*, 106516. [[CrossRef](#)]
17. Hao, G.; Mosey, A.; Jiang, X.; Yost, A.J.; Sapkota, K.R.; Wang, G.T.; Zhang, X.; Zhang, J.; N'Diaye, A.T.; Cheng, R.; et al. Nonvolatile Voltage Controlled Molecular Spin State Switching. *Appl. Phys. Lett.* **2019**, *114*, 032901. [[CrossRef](#)]
18. Miyamachi, T.; Gruber, M.; Davesne, V.; Bowen, M.; Boukari, S.; Joly, L.; Scheurer, F.; Rogez, G.; Yamada, T.K.; Ohresser, P.; et al. Robust Spin Crossover and Memristance across a Single Molecule. *Nat. Commun.* **2012**, *3*, 938. [[CrossRef](#)] [[PubMed](#)]
19. Gopakumar, T.G.; Martino, F.; Naggert, H.; Bannwarth, A.; Tuzcek, F.; Berndt, R. Electron-Induced Spin Crossover of Single Molecules in a Bilayer on Gold. *Angew. Chem. Int. Ed.* **2012**, *51*, 6262–6266. [[CrossRef](#)] [[PubMed](#)]
20. Faulmann, C.; Jacob, K.; Dorbes, S.; Lampert, S.; Malfant, I.; Doublet, M.-L.; Valade, L.; Real, J.A. Electrical Conductivity and Spin Crossover: A New Achievement with a Metal Bis Dithiolene Complex. *Inorg. Chem.* **2007**, *46*, 8548–8559. [[CrossRef](#)]
21. Frisenda, R.; Harzmann, G.D.; Celis Gil, J.A.; Thijssen, J.M.; Mayor, M.; van der Zant, H.S.J. Stretching-Induced Conductance Increase in a Spin-Crossover Molecule. *Nano Lett.* **2016**, *16*, 4733–4737. [[CrossRef](#)]
22. Shvachko, Y.N.; Starichenko, D.V.; Korolyov, A.V.; Yagubskii, E.B.; Kotov, A.I.; Buravov, L.I.; Lysenko, K.A.; Zverev, V.N.; Simonov, S.V.; Zorina, L.V.; et al. The Conducting Spin-Crossover Compound Combining Fe(II) Cation Complex with TCNQ in a Fractional Reduction State. *Inorg. Chem.* **2016**, *55*, 9121–9130. [[CrossRef](#)]
23. Rubio-Giménez, V.; Tatay, S.; Martí-Gastaldo, C. Electrical Conductivity and Magnetic Bistability in Metal–Organic Frameworks and Coordination Polymers: Charge Transport and Spin Crossover at the Nanoscale. *Chem. Soc. Rev.* **2020**, *49*, 5601–5638. [[CrossRef](#)]
24. Wang, M.; Li, Z.-Y.; Ishikawa, R.; Yamashita, M. Spin Crossover and Valence Tautomerism Conductors. *Coord. Chem. Rev.* **2021**, *435*, 213819. [[CrossRef](#)]
25. Takahashi, K.; Cui, H.-B.; Okano, Y.; Kobayashi, H.; Einaga, Y.; Sato, O. Electrical Conductivity Modulation Coupled to a High-Spin–Low-Spin Conversion in the Molecular System [Fe^{III}(Qsal)₂][Ni(Dmit)₂]₃·CH₃CN·H₂O. *Inorg. Chem.* **2006**, *45*, 5739–5741. [[CrossRef](#)] [[PubMed](#)]
26. Lefter, C.; Rat, S.; Costa, J.S.; Manrique-Juárez, M.D.; Quintero, C.M.; Salmon, L.; Séguy, I.; Leichle, T.; Nicu, L.; Demont, P.; et al. Current Switching Coupled to Molecular Spin-States in Large-Area Junctions. *Adv. Mater.* **2016**, *28*, 7508–7514. [[CrossRef](#)] [[PubMed](#)]
27. Shalabaeva, V.; Ridier, K.; Rat, S.; Manrique-Juarez, M.D.; Salmon, L.; Séguy, I.; Rotaru, A.; Molnár, G.; Bousseksou, A. Room Temperature Current Modulation in Large Area Electronic Junctions of Spin Crossover Thin Films. *Appl. Phys. Lett.* **2018**, *112*, 013301. [[CrossRef](#)]
28. Poggini, L.; Gonidec, M.; Canjeevaram Balasubramanyam, R.K.; Squillantini, L.; Pecastaings, G.; Caneschi, A.; Rosa, P. Temperature-Induced Transport Changes in Molecular Junctions Based on a Spin Crossover Complex. *J. Mater. Chem. C* **2019**, *7*, 5343–5347. [[CrossRef](#)]

29. Poggini, L.; Gonidec, M.; González-Estefan, J.H.; Pecastaings, G.; Gobaut, B.; Rosa, P. Vertical Tunnel Junction Embedding a Spin Crossover Molecular Film. *Adv. Electron. Mater.* **2018**, *4*, 1800204. [[CrossRef](#)]
30. Schleicher, F.; Studniarek, M.; Kumar, K.S.; Urbain, E.; Katcko, K.; Chen, J.; Frauhammer, T.; Hervé, M.; Halisdemir, U.; Kandpal, L.M.; et al. Linking Electronic Transport through a Spin Crossover Thin Film to the Molecular Spin State Using X-Ray Absorption Spectroscopy Operando Techniques. *ACS Appl. Mater. Interfaces* **2018**, *10*, 31580–31585. [[CrossRef](#)]
31. Rotaru, A.; Dugay, J.; Tan, R.P.; Gural'skiy, I.A.; Salmon, L.; Demont, P.; Carrey, J.; Molnár, G.; Respaud, M.; Bousseksou, A. Nano-Electromanipulation of Spin Crossover Nanorods: Towards Switchable Nanoelectronic Devices. *Adv. Mater.* **2013**, *25*, 1745–1749. [[CrossRef](#)]
32. Dugay, J.; Giménez-Marqués, M.; Kozlova, T.; Zandbergen, H.W.; Coronado, E.; van der Zant, H.S.J. Spin Switching in Electronic Devices Based on 2D Assemblies of Spin-Crossover Nanoparticles. *Adv. Mater.* **2015**, *27*, 1288–1293. [[CrossRef](#)]
33. Torres-Cavanillas, R.; Sanchis-Gual, R.; Dugay, J.; Coronado-Puchau, M.; Giménez-Marqués, M.; Coronado, E. Design of Bistable Gold@Spin-Crossover Core-Shell Nanoparticles Showing Large Electrical Responses for the Spin Switching. *Adv. Mater.* **2019**, *31*, 1900039. [[CrossRef](#)]
34. Prins, F.; Monrabal-Capilla, M.; Osorio, E.A.; Coronado, E.; van der Zant, H.S.J. Room-Temperature Electrical Addressing of a Bistable Spin-Crossover Molecular System. *Adv. Mater.* **2011**, *23*, 1545–1549. [[CrossRef](#)] [[PubMed](#)]
35. Dugay, J.; Aarts, M.; Giménez-Marqués, M.; Kozlova, T.; Zandbergen, H.W.; Coronado, E.; van der Zant, H.S.J. Phase Transitions in Spin-Crossover Thin Films Probed by Graphene Transport Measurements. *Nano Lett.* **2017**, *17*, 186–193. [[CrossRef](#)] [[PubMed](#)]
36. Holovchenko, A.; Dugay, J.; Giménez-Marqués, M.; Torres-Cavanillas, R.; Coronado, E.; van der Zant, H.S.J. Near Room-Temperature Memory Devices Based on Hybrid Spin-Crossover SiO₂ Nanoparticles Coupled to Single-Layer Graphene Nanoelectrodes. *Adv. Mater.* **2016**, *28*, 7228–7233. [[CrossRef](#)]
37. Zhang, Y.; Séguy, I.; Ridier, K.; Shalabaeva, V.; Piedrahita-Bello, M.; Rotaru, A.; Salmon, L.; Molnár, G.; Bousseksou, A. Resistance Switching in Large-Area Vertical Junctions of the Molecular Spin Crossover Complex [Fe(HB(Tz)₃)₂]: ON/OFF Ratios and Device Stability. *J. Phys. Condens. Matter* **2020**, *32*, 214010. [[CrossRef](#)] [[PubMed](#)]
38. Etrillard, C.; Faramarzi, V.; Dayen, J.-F.; Letard, J.-F.; Doudin, B. Photoconduction in [Fe(Htrz)₂(trz)](BF₄).H₂O Nanocrystals. *Chem. Commun.* **2011**, *47*, 9663. [[CrossRef](#)]
39. Chen, Y.-C.; Meng, Y.; Ni, Z.-P.; Tong, M.-L. Synergistic Electrical Bistability in a Conductive Spin Crossover Heterostructure. *J. Mater. Chem. C* **2015**, *3*, 945–949. [[CrossRef](#)]
40. Tanaka, D.; Aketa, N.; Tanaka, H.; Horike, S.; Fukumori, M.; Tamaki, T.; Inose, T.; Akai, T.; Toyama, H.; Sakata, O.; et al. Facile Preparation of Hybrid Thin Films Composed of Spin-Crossover Nanoparticles and Carbon Nanotubes for Electrical Memory Devices. *Dalton Trans.* **2019**, *48*, 7074–7079. [[CrossRef](#)] [[PubMed](#)]
41. Siddiqui, S.A.; Domanov, O.; Schafler, E.; Vejpravova, J.; Shiozawa, H. Synthesis and Size-Dependent Spin Crossover of Coordination Polymer [Fe(Htrz)₂(trz)](BF₄). *J. Mater. Chem. C* **2021**, *9*, 1077–1084. [[CrossRef](#)]
42. Lefter, C.; Gural'skiy, I.A.; Peng, H.; Molnár, G.; Salmon, L.; Rotaru, A.; Bousseksou, A.; Demont, P. Dielectric and Charge Transport Properties of the Spin Crossover Complex [Fe(Htrz)₂(trz)](BF₄). *Phys. Status Solidi—Rapid Res. Lett. (RRL)* **2014**, *8*, 191–193. [[CrossRef](#)]
43. Ekanayaka, T.K.; Üngör, Ö.; Hu, Y.; Mishra, E.; Phillips, J.P.; Dale, A.S.; Yazdani, S.; Wang, P.; McElveen, K.A.; Zaz, M.Z.; et al. Perturbing the Spin State and Conduction of Fe (II) Spin Crossover Complexes with TCNQ. *Mater. Chem. Phys.* **2023**, *296*, 127276. [[CrossRef](#)]
44. Amin, N.A.A.M.; Said, S.M.; Salleh, M.F.M.; Afifi, A.M.; Ibrahim, N.M.J.N.; Hasnan, M.M.I.M.; Tahir, M.; Hashim, N.Z.I. Review of Fe-Based Spin Crossover Metal Complexes in Multiscale Device Architectures. *Inorganica Chim. Acta* **2023**, *544*, 121168. [[CrossRef](#)]
45. Nieto-Castro, D.; Garcés-Pineda, F.A.; Moneo-Corcuera, A.; Sánchez-Molina, I.; Galán-Mascarós, J.R. Mechanochemical Processing of Highly Conducting Organic/Inorganic Composites Exhibiting Spin Crossover-Induced Memory Effect in Their Transport Properties. *Adv. Funct. Mater.* **2021**, *31*, 2102469. [[CrossRef](#)]
46. Üngör, Ö.; Choi, E.S.; Shatruk, M. Optimization of Crystal Packing in Semiconducting Spin-Crossover Materials with Fractionally Charged TCNQ^{δ-} Anions (0 < δ < 1). *Chem. Sci.* **2021**, *12*, 10765–10779. [[CrossRef](#)]
47. Shvachko, Y.N.; Starichenko, D.V.; Korolyov, A.V.; Kotov, A.I.; Buravov, L.I.; Zverev, V.N.; Simonov, S.V.; Zorina, L.V.; Yagubskii, E.B. The highly conducting spin-crossover compound combining Fe(III) cation complex with TCNQ in a fractional reduction state. Synthesis, structure, electric and magnetic properties. *Magnetochemistry* **2017**, *3*, 9. [[CrossRef](#)]
48. Phan, H.; Benjamin, S.M.; Steven, E.; Brooks, J.S.; Shatruk, M. Photomagnetic Response in Highly Conductive Iron(II) Spin-Crossover Complexes with TCNQ Radicals. *Angew. Chem.* **2015**, *127*, 837–841. [[CrossRef](#)]
49. Yazdani, S.; Collier, K.; Yang, G.; Phillips, J.; Dale, A.; Mosey, A.; Grocki, S.; Zhang, J.; Shanahan, A.E.; Cheng, R.; et al. Optical Characterization of Isothermal Spin State Switching in an Fe (II) Spin Crossover Molecular and Polymer Ferroelectric Bilayer. *J. Phys. Condens. Matter* **2023**, *35*, 365401. [[CrossRef](#)]
50. Costa, P.; Hao, G.; N'Diaye, A.T.; Routaboul, L.; Braunstein, P.; Zhang, X.; Zhang, J.; Doudin, B.; Enders, A.; Dowben, P.A. Perturbing the Spin Crossover Transition Activation Energies in [Fe(H₂B(pz)₂)₂(bipy)] with Zwitterionic Additions. *J. Phys. Condens. Matter* **2018**, *30*, 305503. [[CrossRef](#)] [[PubMed](#)]
51. Costa, P.S.; Hao, G.; N'Diaye, A.T.; Routaboul, L.; Braunstein, P.; Zhang, X.; Zhang, J.; Ekanayaka, T.K.; Shi, Q.-Y.; Schlegel, V.; et al. Manipulation of the Molecular Spin Crossover Transition of [Fe(H₂B(pz)₂)₂(bipy)] by Addition of Polar Molecules. *J. Phys. Condens. Matter* **2020**, *32*, 034001. [[CrossRef](#)] [[PubMed](#)]

52. Zhang, X.; Costa, P.S.; Hooper, J.; Miller, D.P.; N'Diaye, A.T.; Beniwal, S.; Jiang, X.; Yin, Y.; Rosa, P.; Routaboul, L.; et al. Locking and Unlocking the Molecular Spin Crossover Transition. *Adv. Mater.* **2017**, *29*, 1702257. [[CrossRef](#)]
53. Zhang, X.; Mu, S.; Chastanet, G.; Daro, N.; Palamarciuc, T.; Rosa, P.; Létard, J.-F.; Liu, J.; Sterbinsky, G.E.; Arena, D.A.; et al. Complexities in the Molecular Spin Crossover Transition. *J. Phys. Chem. C* **2015**, *119*, 16293–16302. [[CrossRef](#)]
54. Zhang, X.; Palamarciuc, T.; Rosa, P.; Létard, J.-F.; Doudin, B.; Zhang, Z.; Wang, J.; Dowben, P.A. Electronic Structure of a Spin Crossover Molecular Adsorbate. *J. Phys. Chem. C* **2012**, *116*, 23291–23296. [[CrossRef](#)]
55. Moliner, N.; Salmon, L.; Capes, L.; Muñoz, M.C.; Létard, J.-F.; Bousseksou, A.; Tuchagues, J.-P.; McGarvey, J.J.; Dennis, A.C.; Castro, M.; et al. Thermal and Optical Switching of Molecular Spin States in the $\{[\text{FeL}[\text{H}_2\text{B}(\text{pz})_2]_2\}$ Spin-Crossover System (L = Bpy, Phen). *J. Phys. Chem. B* **2002**, *106*, 4276–4283. [[CrossRef](#)]
56. Zhang, X.; Palamarciuc, T.; Létard, J.-F.; Rosa, P.; Lozada, E.V.; Torres, F.; Rosa, L.G.; Doudin, B.; Dowben, P.A. The Spin State of a Molecular Adsorbate Driven by the Ferroelectric Substrate Polarization. *Chem. Commun.* **2014**, *50*, 2255. [[CrossRef](#)]
57. Yazdani, S.; Phillips, J.; Ekanayaka, T.K.; Cheng, R.; Dowben, P.A. The Influence of the Substrate on the Functionality of Spin Crossover Molecular Materials. *Molecules* **2023**, *28*, 3735. [[CrossRef](#)]
58. Ekanayaka, T.K.; Kurz, H.; Dale, A.S.; Hao, G.; Mosey, A.; Mishra, E.; N'Diaye, A.T.; Cheng, R.; Weber, B.; Dowben, P.A. Probing the Unpaired Fe Spins across the Spin Crossover of a Coordination Polymer. *Mater. Adv.* **2021**, *2*, 760–768. [[CrossRef](#)]
59. Bousseksou, A.; Molnár, G.; Demont, P.; Menegotto, J. Observation of a Thermal Hysteresis Loop in the Dielectric Constant of Spin Crossover Complexes: Towards Molecular Memory Devices. *J. Mater. Chem.* **2003**, *13*, 2069–2071. [[CrossRef](#)]
60. Pavlik, J.; Linares, J. Microscopic Models of Spin Crossover. *Comptes Rendus Chim.* **2018**, *21*, 1170–1178. [[CrossRef](#)]
61. Hao, G.; Dale, A.S.; N'Diaye, A.T.; Chopdekar, R.V.; Koch, R.J.; Jiang, X.; Mellinger, C.; Zhang, J.; Cheng, R.; Xu, X.; et al. Intermolecular Interaction and Cooperativity in an Fe (II) Spin Crossover Molecular Thin Film System. *J. Phys. Condens. Matter* **2022**, *34*, 295201. [[CrossRef](#)]
62. Konishi, Y.; Tokoro, H.; Nishino, M.; Miyashita, S. Monte Carlo Simulation of Pressure-Induced Phase Transitions in Spin-Crossover Materials. *Phys. Rev. Lett.* **2008**, *100*, 067206. [[CrossRef](#)]
63. Ishikawa, R.; Ueno, S.; Nifuku, S.; Horii, Y.; Iguchi, H.; Miyazaki, Y.; Nakano, M.; Hayami, S.; Kumagai, S.; Katoh, K.; et al. Simultaneous Spin-Crossover Transition and Conductivity Switching in a Dinuclear Iron(II) Coordination Compound Based on 7,7',8,8'-Tetracyano-*p*-quinodimethane. *Chem.–A Eur. J.* **2020**, *26*, 1278–1285. [[CrossRef](#)]
64. Stoleriu, L.; Nishino, M.; Miyashita, S.; Stancu, A.; Hauser, A.; Enachescu, C. Cluster Evolution in Molecular Three-Dimensional Spin-Crossover Systems. *Phys. Rev. B* **2017**, *96*, 064115. [[CrossRef](#)]
65. Dankhoff, K.; Lochenie, C.; Weber, B. Iron (II) Spin Crossover Complexes with 4,4'-Dipyridylethyne—Crystal Structures and Spin Crossover with Hysteresis. *Molecules* **2020**, *25*, 581. [[CrossRef](#)] [[PubMed](#)]
66. Bauer, W.; Lochenie, C.; Weber, B. Synthesis and Characterization of 1D Iron (II) Spin Crossover Coordination Polymers with Hysteresis. *Dalton Trans.* **2014**, *43*, 1990–1999. [[CrossRef](#)]
67. Bauer, W.; Schlamp, S.; Weber, B. A Ladder Type Iron (II) Coordination Polymer with Cooperative Spin Transition. *Chem. Commun.* **2012**, *48*, 10222. [[CrossRef](#)]
68. Li, Q.; Li, Z. Molecular Packing: Another Key Point for the Performance of Organic and Polymeric Optoelectronic Materials. *Acc. Chem. Res.* **2020**, *53*, 962–973. [[CrossRef](#)] [[PubMed](#)]
69. Chen, S.; Ma, J. Substituent Effects on Packing Entropy and Film Morphologies in the Nucleation of Functionalized Pentacenes on SiO₂ Substrate: Molecular Dynamics Simulations. *J. Chem. Phys.* **2012**, *137*, 074708. [[CrossRef](#)]
70. Gentili, D.; Sonar, P.; Liscio, F.; Cramer, T.; Ferlauto, L.; Leonardi, F.; Milita, S.; Dodabalapur, A.; Cavallini, M. Logic-Gate Devices Based on Printed Polymer Semiconducting Nanostripes. *Nano Lett.* **2013**, *13*, 3643–3647. [[CrossRef](#)] [[PubMed](#)]
71. Nawaz, A.; Tavares, A.C.B.; Trang Do, T.; Patil, B.B.; Sonar, P.; Hümmelgen, I.A. Experimental and Modeling Study of Low-Voltage Field-Effect Transistors Fabricated with Molecularly Aligned Copolymer Floating Films. *Flex. Print. Electron.* **2018**, *3*, 015006. [[CrossRef](#)]
72. Aleeva, Y.; Pignataro, B. Recent Advances in Upscalable Wet Methods and Ink Formulations for Printed Electronics. *J. Mater. Chem. C* **2014**, *2*, 6436–6453. [[CrossRef](#)]
73. Craze, A.R.; Marjo, C.E.; Li, F. A Complementary Characterisation Technique for Spin Crossover Materials; the Application of X-Ray Photoelectron Spectroscopy for Future Device Applications. *Dalton Trans.* **2022**, *51*, 428–441. [[CrossRef](#)] [[PubMed](#)]
74. Bairagi, K.; Iasco, O.; Bellec, A.; Kartsev, A.; Li, D.; Lagoute, J.; Chacon, C.; Girard, Y.; Rousset, S.; Miserque, F.; et al. Molecular-Scale Dynamics of Light-Induced Spin Cross-over in a Two-Dimensional Layer. *Nat. Commun.* **2016**, *7*, 12212. [[CrossRef](#)] [[PubMed](#)]
75. Zhang, X.; N'Diaye, A.T.; Jiang, X.; Zhang, X.; Yin, Y.; Chen, X.; Hong, X.; Xu, X.; Dowben, P.A. Indications of Magnetic Coupling Effects in Spin Cross-over Molecular Thin Films. *Chem. Commun.* **2018**, *54*, 944–947. [[CrossRef](#)] [[PubMed](#)]
76. Beniwal, S.; Zhang, X.; Mu, S.; Naim, A.; Rosa, P.; Chastanet, G.; Létard, J.-F.; Liu, J.; Sterbinsky, G.E.; Arena, D.A.; et al. Surface-Induced Spin State Locking of the $[\text{Fe}(\text{H}_2\text{B}(\text{pz})_2)_2(\text{bipy})]$ Spin Crossover Complex. *J. Phys. Condens. Matter* **2016**, *28*, 206002. [[CrossRef](#)] [[PubMed](#)]
77. Hao, G.; N'Diaye, A.T.; Ekanayaka, T.K.; Dale, A.S.; Jiang, X.; Mishra, E.; Mellinger, C.; Yazdani, S.; Freeland, J.W.; Zhang, J.; et al. Magnetic Field Perturbations to a Soft X-Ray-Activated Fe (II) Molecular Spin State Transition. *Magnetochemistry* **2021**, *7*, 135. [[CrossRef](#)]

78. Warner, B.; Oberg, J.C.; Gill, T.G.; El Hallak, F.; Hirjibehedin, C.F.; Serri, M.; Heutz, S.; Arrio, M.-A.; Sainctavit, P.; Mannini, M.; et al. Temperature- and Light-Induced Spin Crossover Observed by X-Ray Spectroscopy on Isolated Fe (II) Complexes on Gold. *J. Phys. Chem. Lett.* **2013**, *4*, 1546–1552. [[CrossRef](#)]
79. Ishii, H.; Sugiyama, K.; Ito, E.; Seki, K. Energy Level Alignment and Interfacial Electronic Structures at Organic/Metal and Organic/Organic Interfaces. *Adv. Mater.* **1999**, *22*, 605–625. [[CrossRef](#)]
80. Braun, S.; Salaneck, W.R.; Fahlman, M. Energy-Level Alignment at Organic/Metal and Organic/Organic Interfaces. *Adv. Mater.* **2009**, *21*, 1450–1472. [[CrossRef](#)]
81. Dowben, P.A. The Metallicity of Thin Films and Overlayers. *Surf. Sci. Rept.* **2000**, *40*, 151–247. [[CrossRef](#)]

Disclaimer/Publisher's Note: The statements, opinions and data contained in all publications are solely those of the individual author(s) and contributor(s) and not of MDPI and/or the editor(s). MDPI and/or the editor(s) disclaim responsibility for any injury to people or property resulting from any ideas, methods, instructions or products referred to in the content.